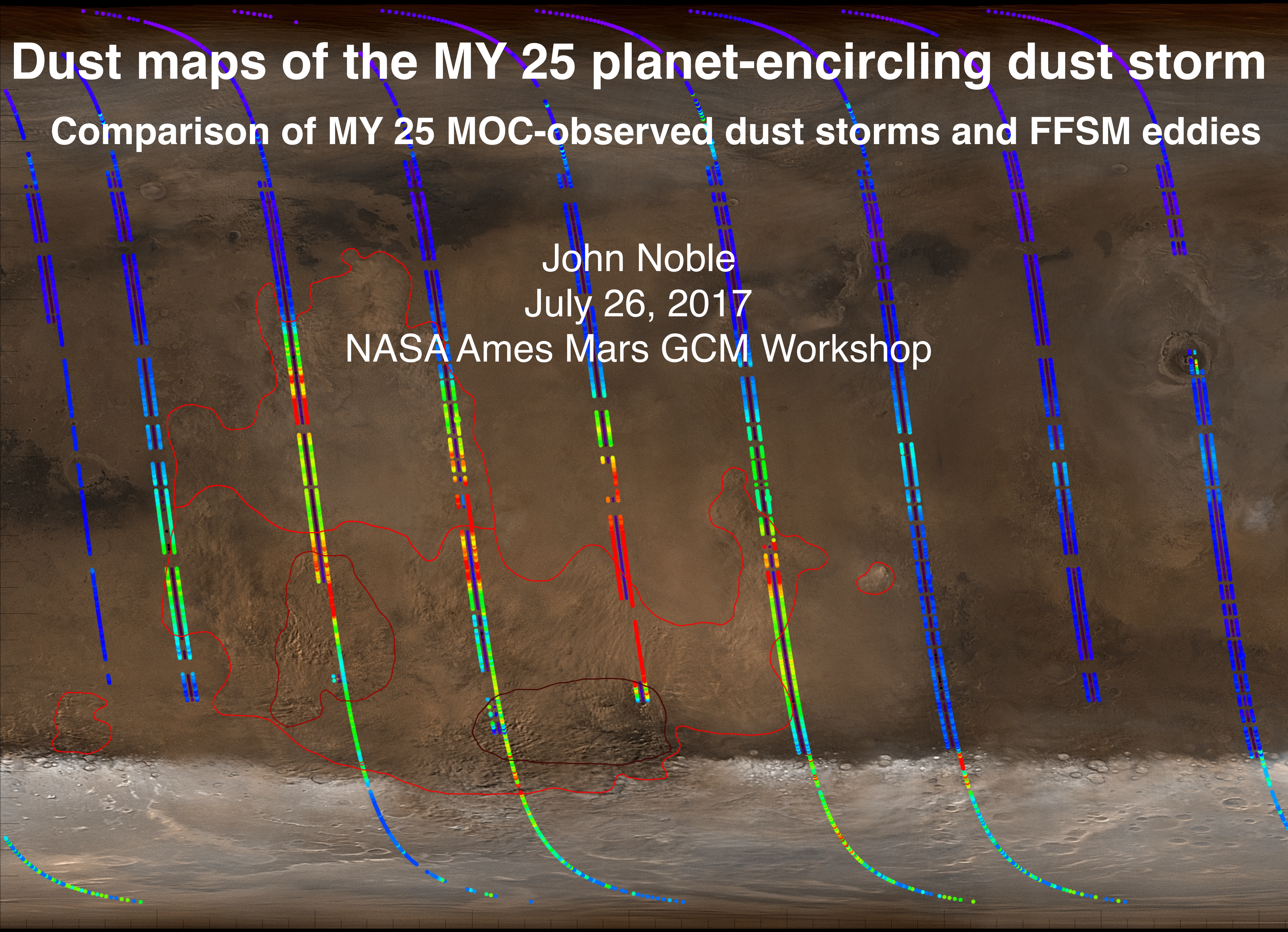

Dust maps of the MY 25 planet-encircling dust storm

Comparison of MY 25 MOC-observed dust storms and FFSM eddies

John Noble
July 26, 2017
NASA Ames Mars GCM Workshop

Outline

- Motivation
- Methods
  - Dust characterization scheme
  - Map development
- Results
  - Comparison of eddy and dust storm migration
    - Velocity
    - Periodicity
- Working Hypothesis
- Discussion

Motivation

- TES opacity retrieval reliability is partially a function of ground-air temperature contrast, with reliability diminishing as contrast approaches zero. Contrast limits occur at high-latitudes (>55°N, <60°S), and in extremely dusty conditions. Significant portions of the TES retrievals are missing or unreliable due to high opacity levels and diminished contrast.

- Better delimit the areal extent of MOC-observed dust storms for eddy and storm analysis, since previous comparison of MOC-observed dust storms and FFSM eddies was imprecise latitudinally

- Provide improved input to GCM

Dust characterization scheme

	Aerosol activity		**Dust storm & dust cloud**
Structure	Dust storms	Ripple patterns	Description & features
3	113	313	Structure = high • large lobes and plumes • strong shadows & contrast
2	112	312	Structure = medium • medium lobes and plumes • medium shadows & contrast
1	111	311	Structure = low • small lobes; small plumes in craters • weak shadows & contrast
0	110	N/A	Structure = none/minimal • no lobate features • no/minimal shadows & contrast

Ripple patterns (dust entrained in gravity waves)

- Included for completeness - not used in FFSM analysis
- May indicate dust transport

Map development

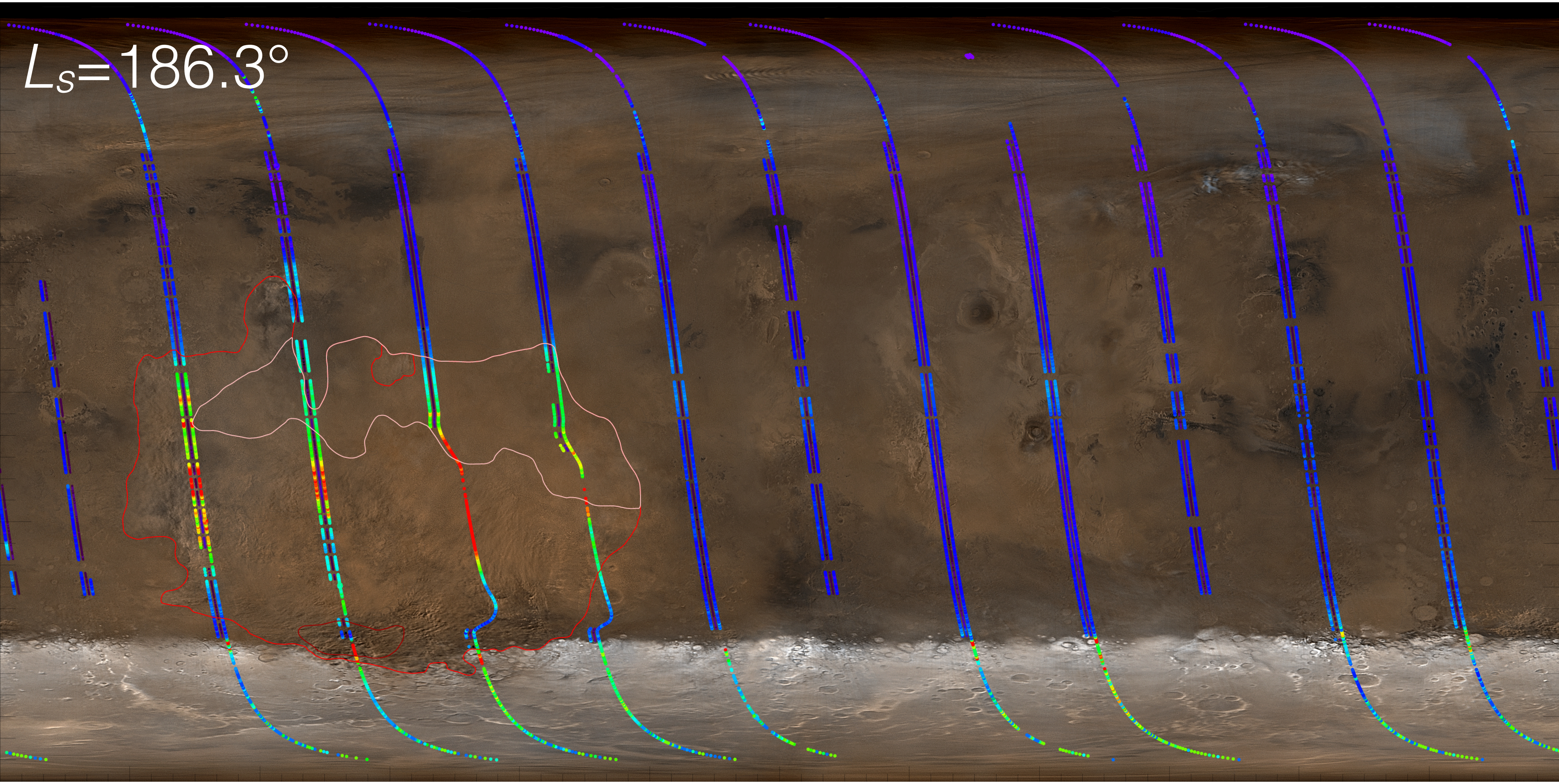

- Groundtracks: 1) TES 9-µm dust opacity
  2) TES water ice opacity
  3) GCM-derived dust opacity (Wilson *et al.* 2011)

Ls=177.4

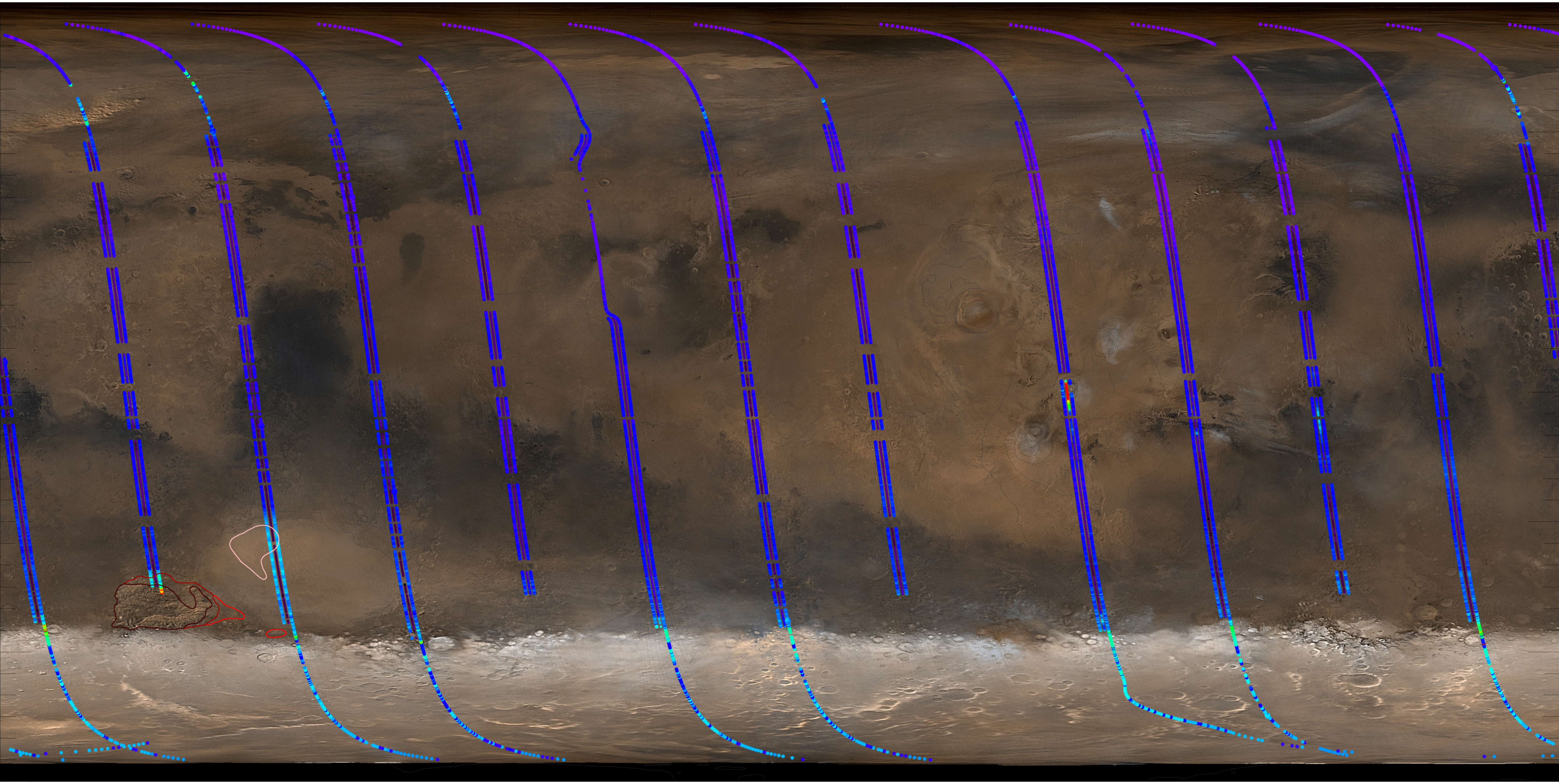

Ls=178.0

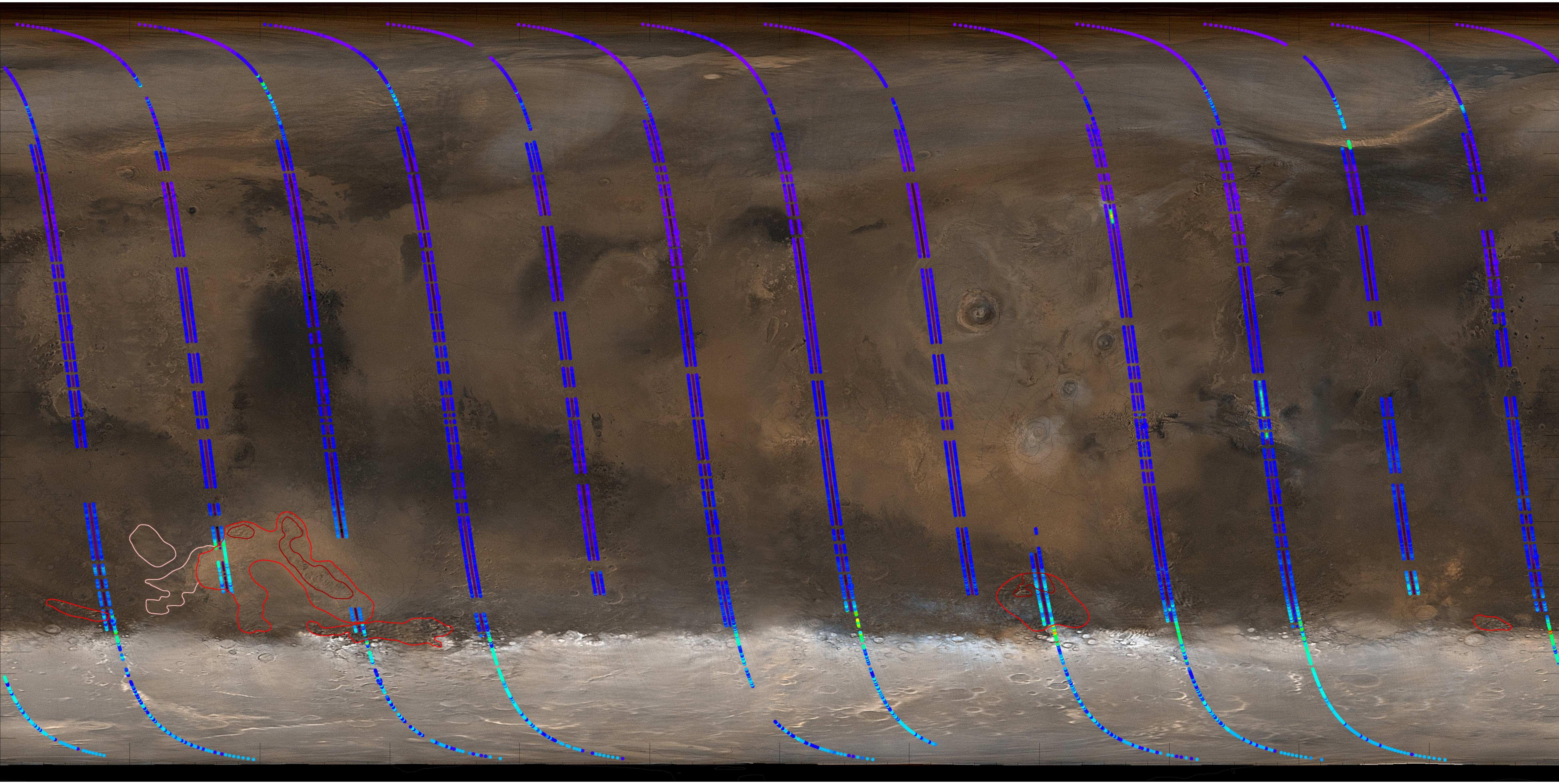

Ls=178.0

Storm Catalog

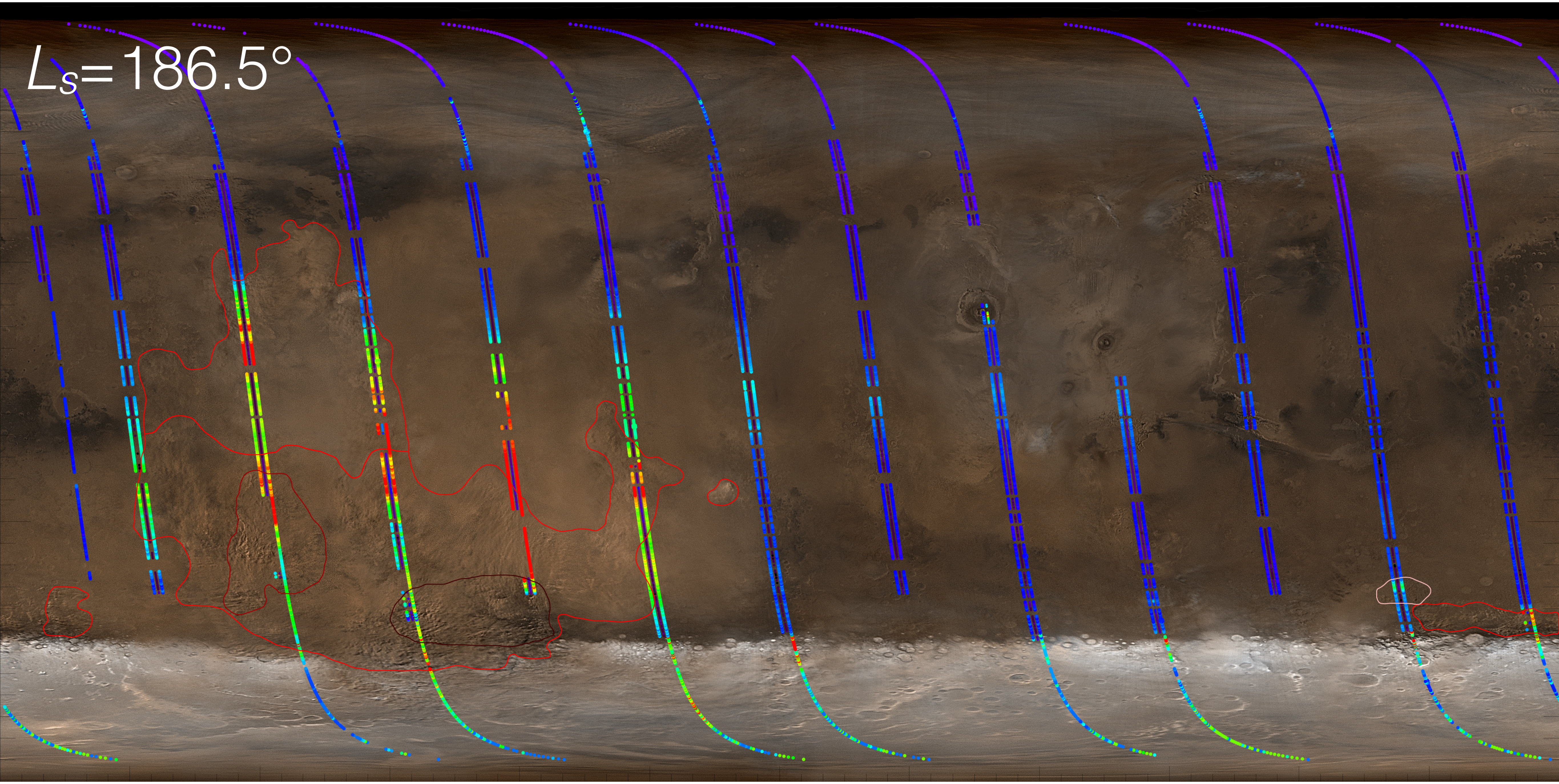

- Identifies storms by lat/lon coordinates, and MOC ID
- Catalogs duplicate storms (in MOC imagery)
  - duplicates appear on ~ 1/3 of DGMs

Storm Catalog

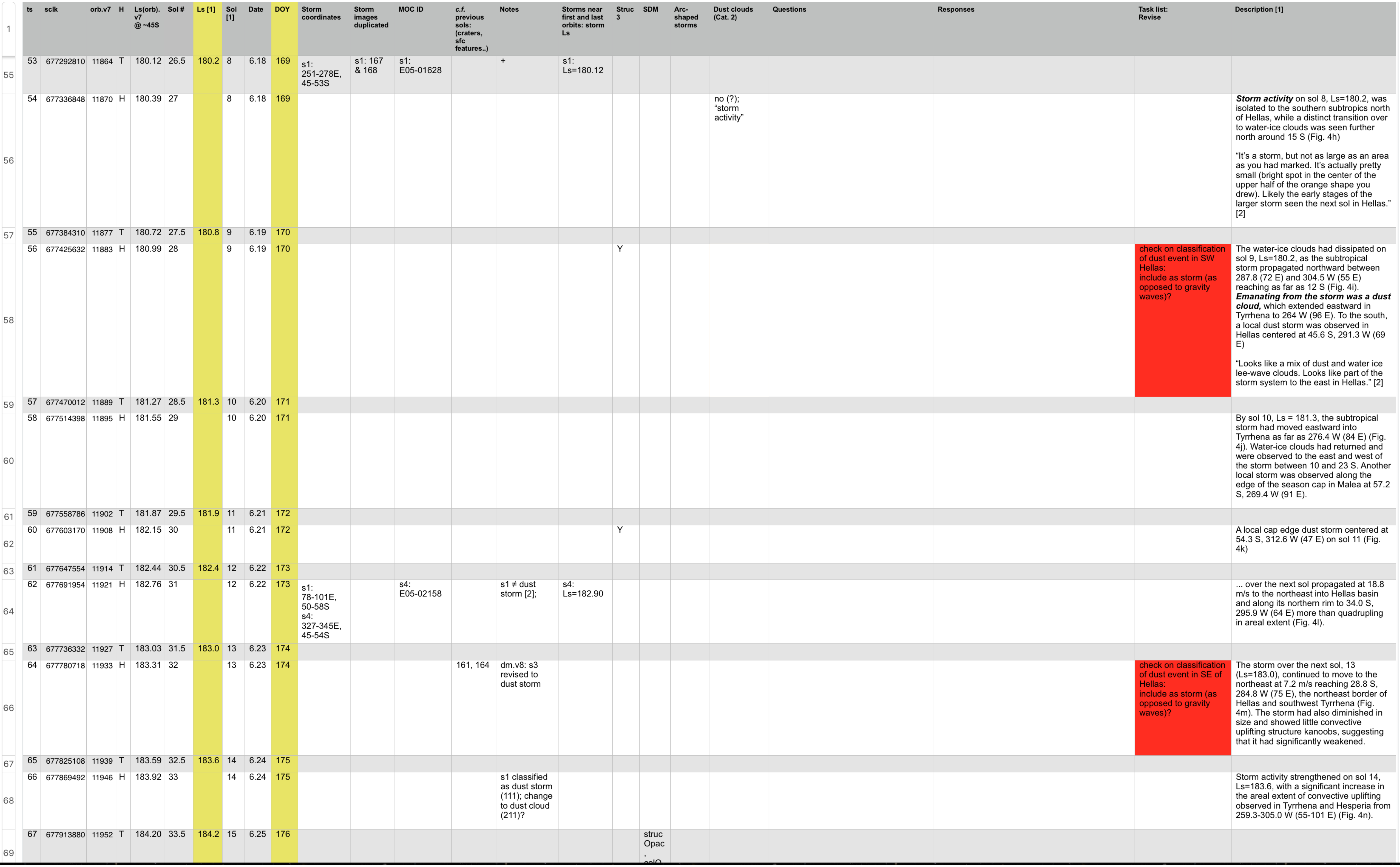

1	ts	sclk	orb.v7	H	Ls(orb). v7 @ ~45S	Sol #	Ls [1]	Sol [1]	Date	DOY	Storm coordinates	Storm images duplicated	MOC ID	*c.f.* previous sols: (craters, sfc features..)	Notes	Storms near first and last orbits: storm Ls	Struc 3	SDM	Arc-shaped storms	Dust clouds (Cat. 2)	Questions	Responses	Task list: Revise	Description [1]
55	53	677292810	11864	T	180.12	26.5	180.2	8	6.18	169	s1: 251-278E, 45-53S	s1: 167 & 168	s1: E05-01628		+	s1: Ls=180.12								
56	54	677336848	11870	H	180.39	27		8	6.18	169										no (?); “storm activity”				***Storm activity*** on sol 8, Ls=180.2, was isolated to the southern subtropics north of Hellas, while a distinct transition over to water-ice clouds was seen further north around 15 S (Fig. 4h) “It’s a storm, but not as large as an area as you had marked. It’s actually pretty small (bright spot in the center of the upper half of the orange shape you drew). Likely the early stages of the larger storm seen the next sol in Hellas.” [2]
57	55	677384310	11877	T	180.72	27.5	180.8	9	6.19	170														
58	56	677425632	11883	H	180.99	28		9	6.19	170							Y						check on classification of dust event in SW Hellas: include as storm (as opposed to gravity waves)?	The water-ice clouds had dissipated on sol 9, Ls=180.2, as the subtropical storm propagated northward between 287.8 (72 E) and 304.5 W (55 E) reaching as far as 12 S (Fig. 4i). ***Emanating from the storm was a dust cloud,*** which extended eastward in Tyrrhena to 264 W (96 E). To the south, a local dust storm was observed in Hellas centered at 45.6 S, 291.3 W (69 E) “Looks like a mix of dust and water ice lee-wave clouds. Looks like part of the storm system to the east in Hellas.” [2]
59	57	677470012	11889	T	181.27	28.5	181.3	10	6.20	171														
60	58	677514398	11895	H	181.55	29		10	6.20	171														By sol 10, Ls = 181.3, the subtropical storm had moved eastward into Tyrrhena as far as 276.4 W (84 E) (Fig. 4j). Water-ice clouds had returned and were observed to the east and west of the storm between 10 and 23 S. Another local storm was observed along the edge of the season cap in Malea at 57.2 S, 269.4 W (91 E).
61	59	677558786	11902	T	181.87	29.5	181.9	11	6.21	172														
62	60	677603170	11908	H	182.15	30		11	6.21	172							Y							A local cap edge dust storm centered at 54.3 S, 312.6 W (47 E) on sol 11 (Fig. 4k)
63	61	677647554	11914	T	182.44	30.5	182.4	12	6.22	173														
64	62	677691954	11921	H	182.76	31		12	6.22	173	s1: 78-101E, 50-58S s4: 327-345E, 45-54S		s4: E05-02158		s1 ≠ dust storm [2];	s4: Ls=182.90								... over the next sol propagated at 18.8 m/s to the northeast into Hellas basin and along its northern rim to 34.0 S, 295.9 W (64 E) more than quadrupling in areal extent (Fig. 4l).
65	63	677736332	11927	T	183.03	31.5	183.0	13	6.23	174														
66	64	677780718	11933	H	183.31	32		13	6.23	174				161, 164	dm.v8: s3 revised to dust storm								check on classification of dust event in SE of Hellas: include as storm (as opposed to gravity waves)?	The storm over the next sol, 13 (Ls=183.0), continued to move to the northeast at 7.2 m/s reaching 28.8 S, 284.8 W (75 E), the northeast border of Hellas and southwest Tyrrhena (Fig. 4m). The storm had also diminished in size and showed little convective uplifting structure kanoobs, suggesting that it had significantly weakened.
67	65	677825108	11939	T	183.59	32.5	183.6	14	6.24	175														
68	66	677869492	11946	H	183.92	33		14	6.24	175					s1 classified as dust storm (111); change to dust cloud (211)?									Storm activity strengthened on sol 14, Ls=183.6, with a significant increase in the areal extent of convective uplifting observed in Tyrrhena and Hesperia from 259.3-305.0 W (55-101 E) (Fig. 4n).
69	67	677913880	11952	T	184.20	33.5	184.2	15	6.25	176								struc Opac ,						

Fast Fourier Synoptic Mapping

Fast Fourier Synoptic Mapping (FFSM) is a spectral analysis method that creates synoptic maps from asynoptic data, maintaining full space-time resolution without distorting or smoothing higher frequency (~1–3 sols) weather signals (Barnes 2001, 2003, 2006).

This process removes the time mean, zonal mean, and westward diurnal tide.

Due to the time domain (40 sols) which covers the transition from winter to spring, we removed the seasonal slope/trend:

$y(t)$ = original time series
$z(t)$ = linear trend (seasonal)
$w(t) = y(t) - z(t)$

Trend was removed from each 5-deg longitude grid cell

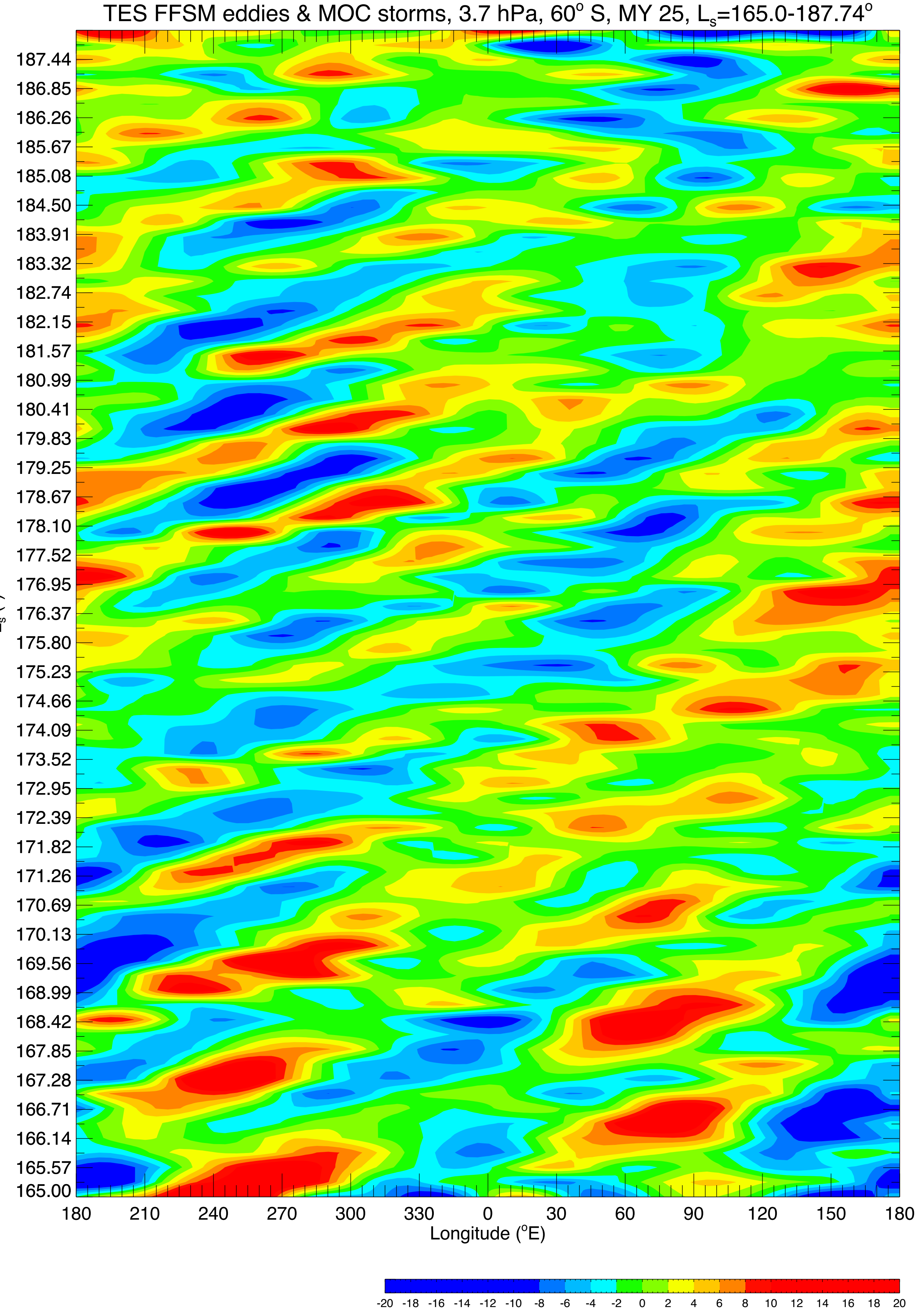

TES FFSM eddies & MOC storms, 3.7 hPa, 60° S, MY 25, L_s=165.0-187.74°

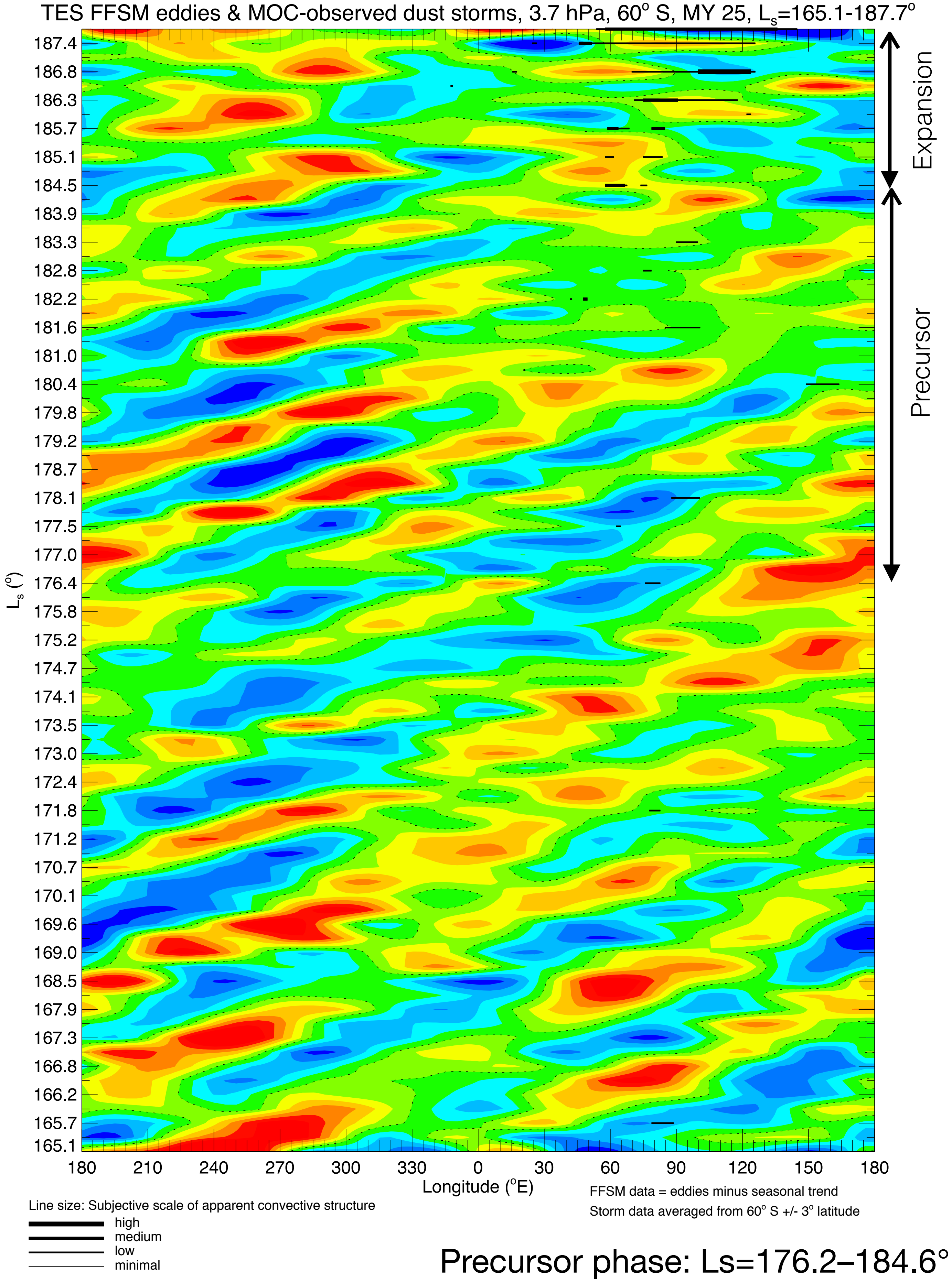

TES FFSM eddies & MOC-observed dust storms, 3.7 hPa, 60° S, MY 25, L_s=165.1-187.7°

FFSM data = eddies minus seasonal trend

Storm data averaged from 60° S +/- 3° latitude

Precursor phase: Ls=176.2–184.6°

Expansion phase: Ls=184.7–200.3°

Eddies & storm evolution

FFSM analysis of TES temperatures (Barnes 2006) has shown that fourteen cold waves (E1–E14) propagated through Hellas from L_s=165–188.

- E7–E12 occurred during the precursor phase (L_s=176.2–184.6°)
- E13 and E14 during the expansion phase (L_s=184.7–200.3°)

Precursor phase: L_s=176.2–184.6°

Expansion phase: L_s=184.7–200.3°

TES FFSM eddies & MOC-observed dust storms, 3.7 hPa, 55° S, MY 25, L_s=165.1-187.7

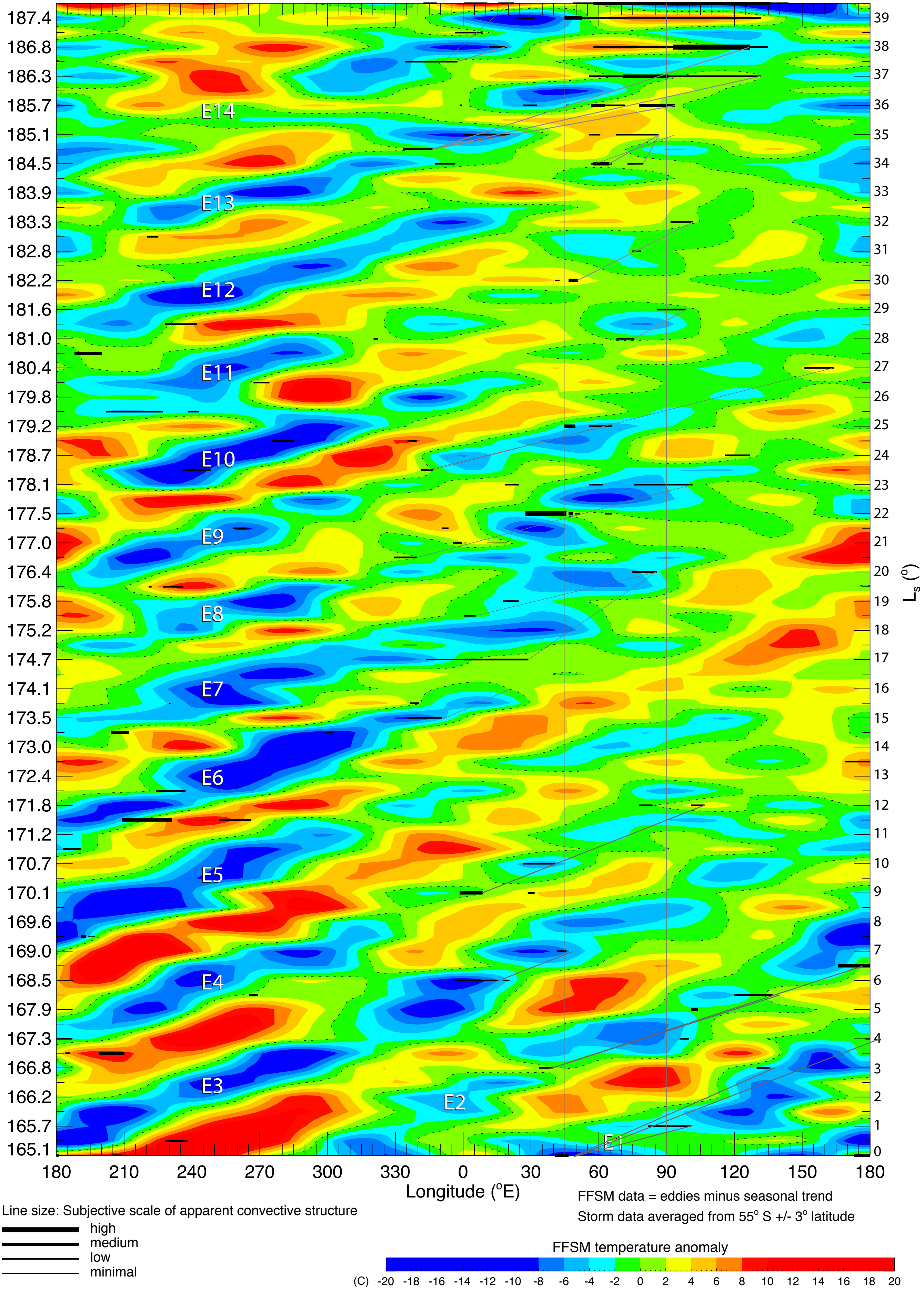

TES FFSM eddies & MOC-observed dust storms, 3.7 hPa, 50° S, MY 25, L_s=165.1-187.7°

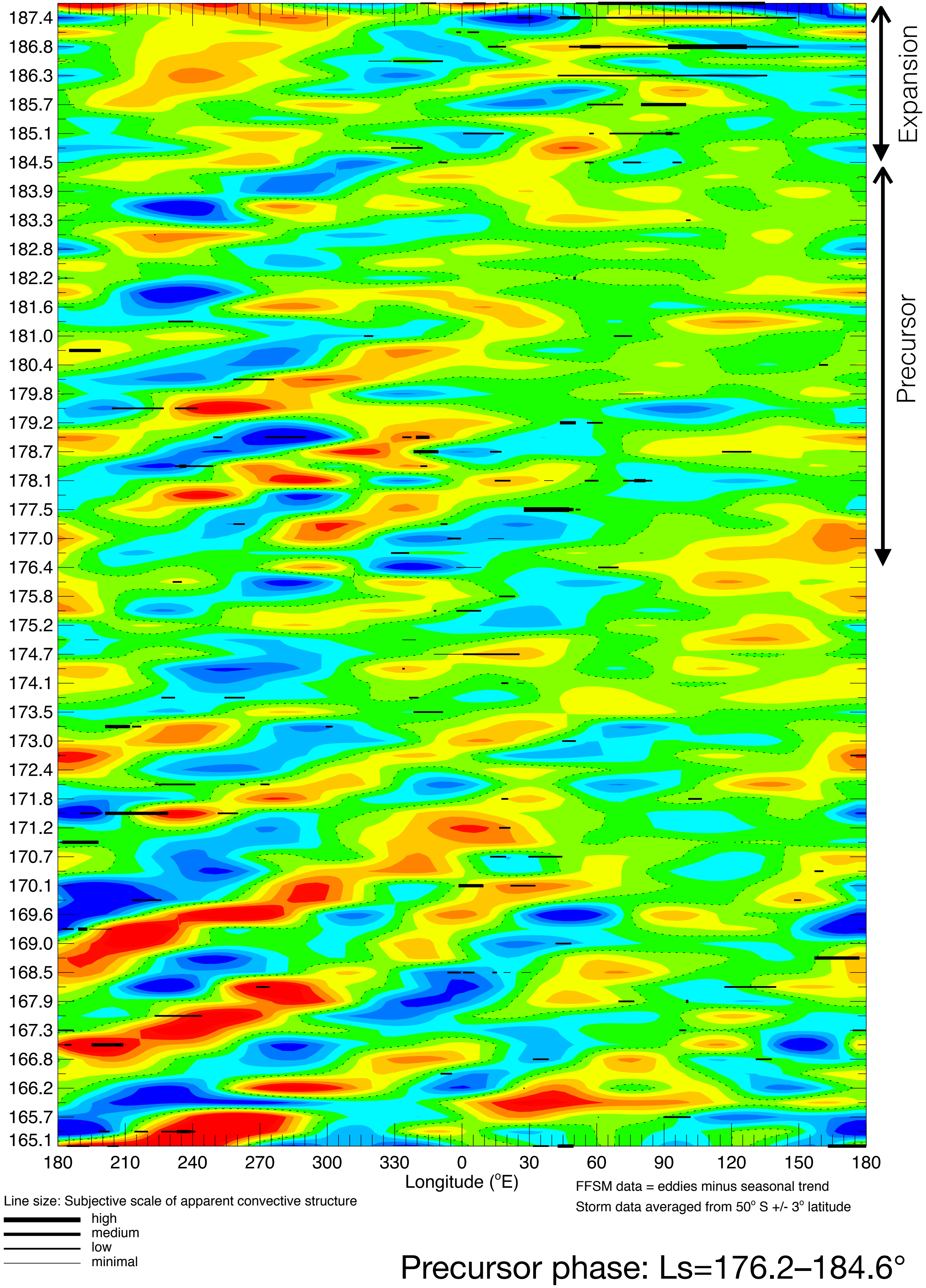

Precursor phase: Ls=176.2–184.6°

Expansion phase: Ls=184.7–200.3°

Eddy vertical structure

Eddy structure near Hellas at 60 S (Ls =173–184) changes with height.

- 3.7–1.36 hPa: high amplitude cold anomalies
- 0.5 hPa: warm anomalies
- 0.1 hPa: high amplitude warm anomalies

This change in eddy structure with height indicates that these are baroclinic (not barotropic) eddies

Eddy vertical structure

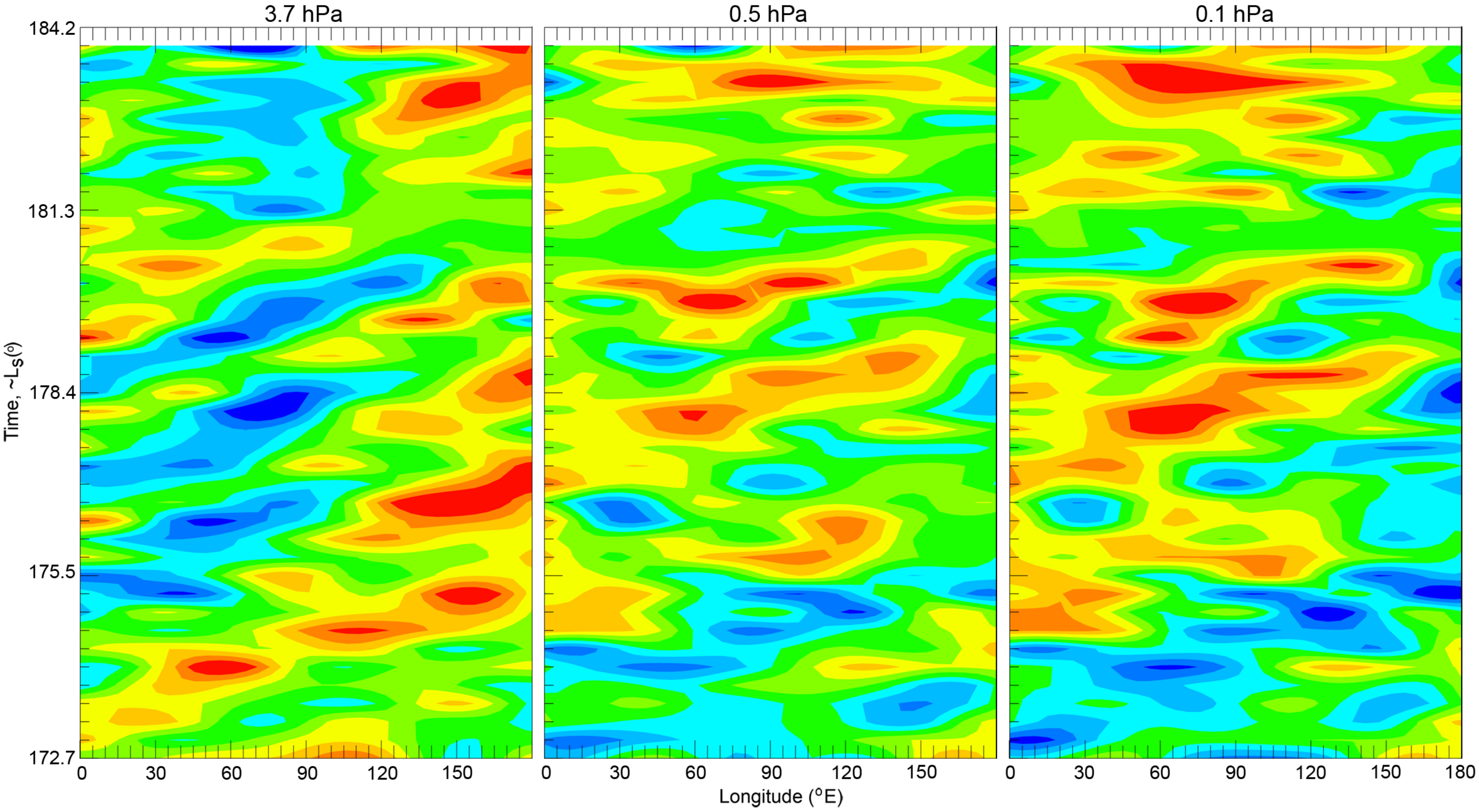

Migration velocity

Eddy phase speed

We subjectively defined globally-coherent eddies and calculated their phase speed, c, using:

$c(x) = \Delta x / \Delta t$, where $\Delta x = (r_{eq} \cdot \cos\phi) \cdot \Delta\lambda$,
r_{eq} is planetary radius, ϕ is latitude, λ is longitude, and t is time at 180° E.

Storm migration speed

Calculated using eastern edge of storm

TES FFSM eddies & MOC-observed dust storms, 3.7 hPa, 55^o S, MY 25, L_s=165.1-187.7

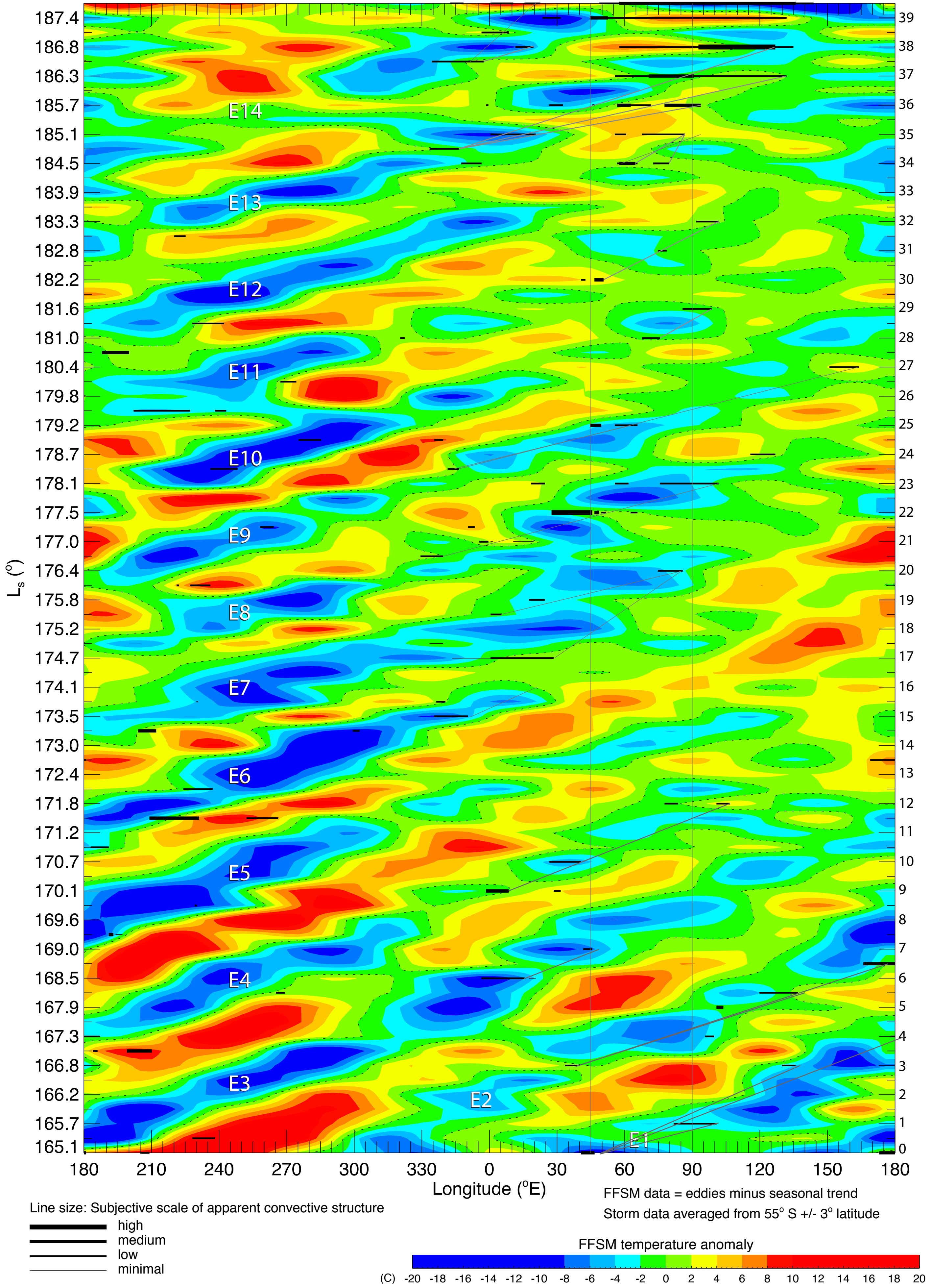

FFSM data = eddies minus seasonal trend

Storm data averaged from 55^o S +/- 3^o latitude

Migration speed – eddies & storms

Eddy #	Eddy phase speed, *c* (m/s), (55S; global)	Eddy phase speed, *c* (m/s), (55S; 0–120E)	Storm migration speed, *v* (m/s), 55 S	Storm migration speed, *v* (m/s), 50 S
1	—	—		12.6
2	13.3	12.8		17.2
3	14.6	11.8		14.2
4	16.1	12.6	12.5	
5	15.9	17.7		—
6	17.7	15.3		12.5
7	16.2	12.8	7.3	
8	16.8	13.5	18.7	
9	16.0	14.4	19.4	
10	15.5	14.8	8.8	
11	15.2	12.4	9.8	
12	—	15.3		15.0
13	—	12.8	15.3	24.9
14	—	—		5.0

Migration speed of eddies (global) & dust storms

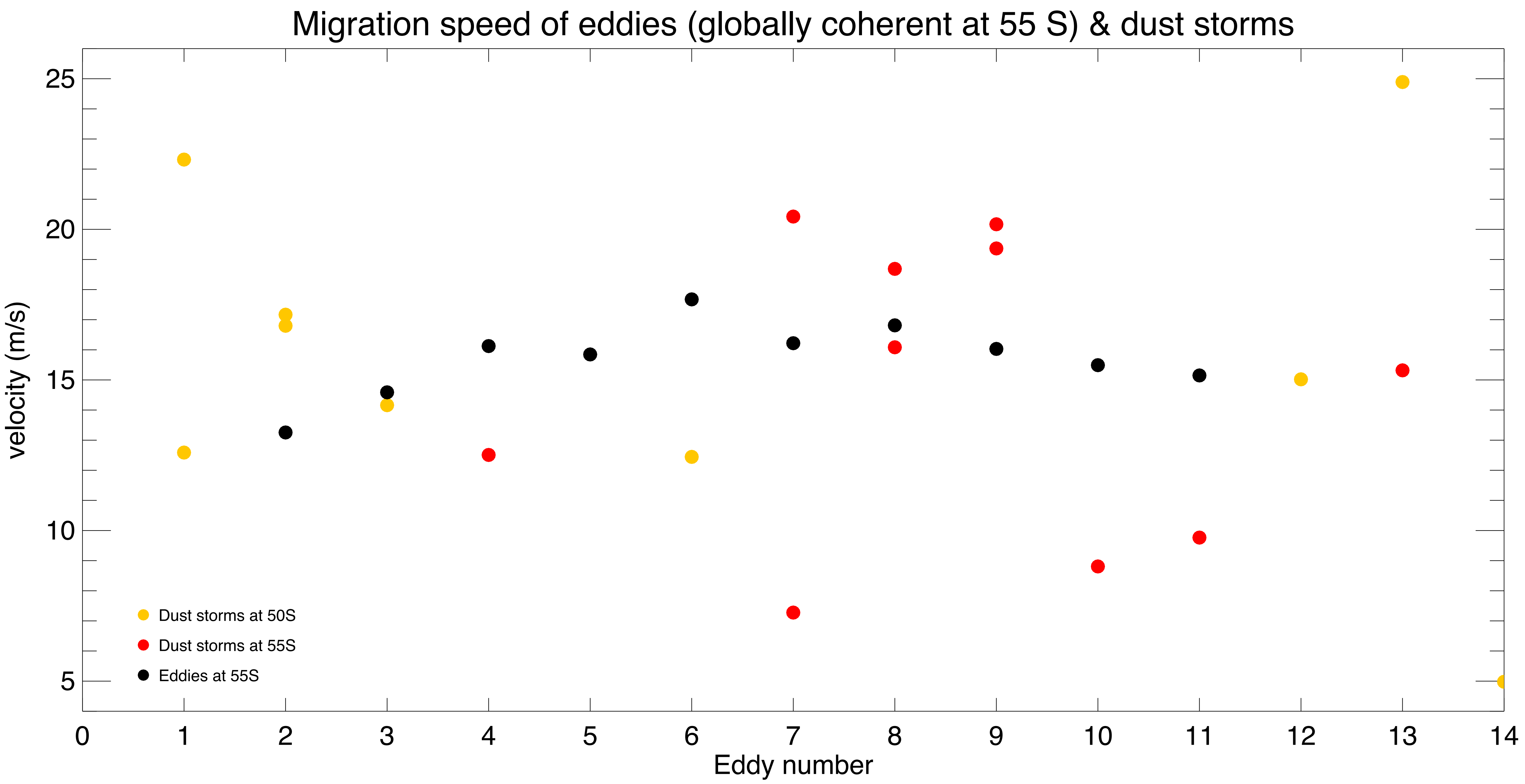

Migration speed of eddies (0–120 E) & dust storms

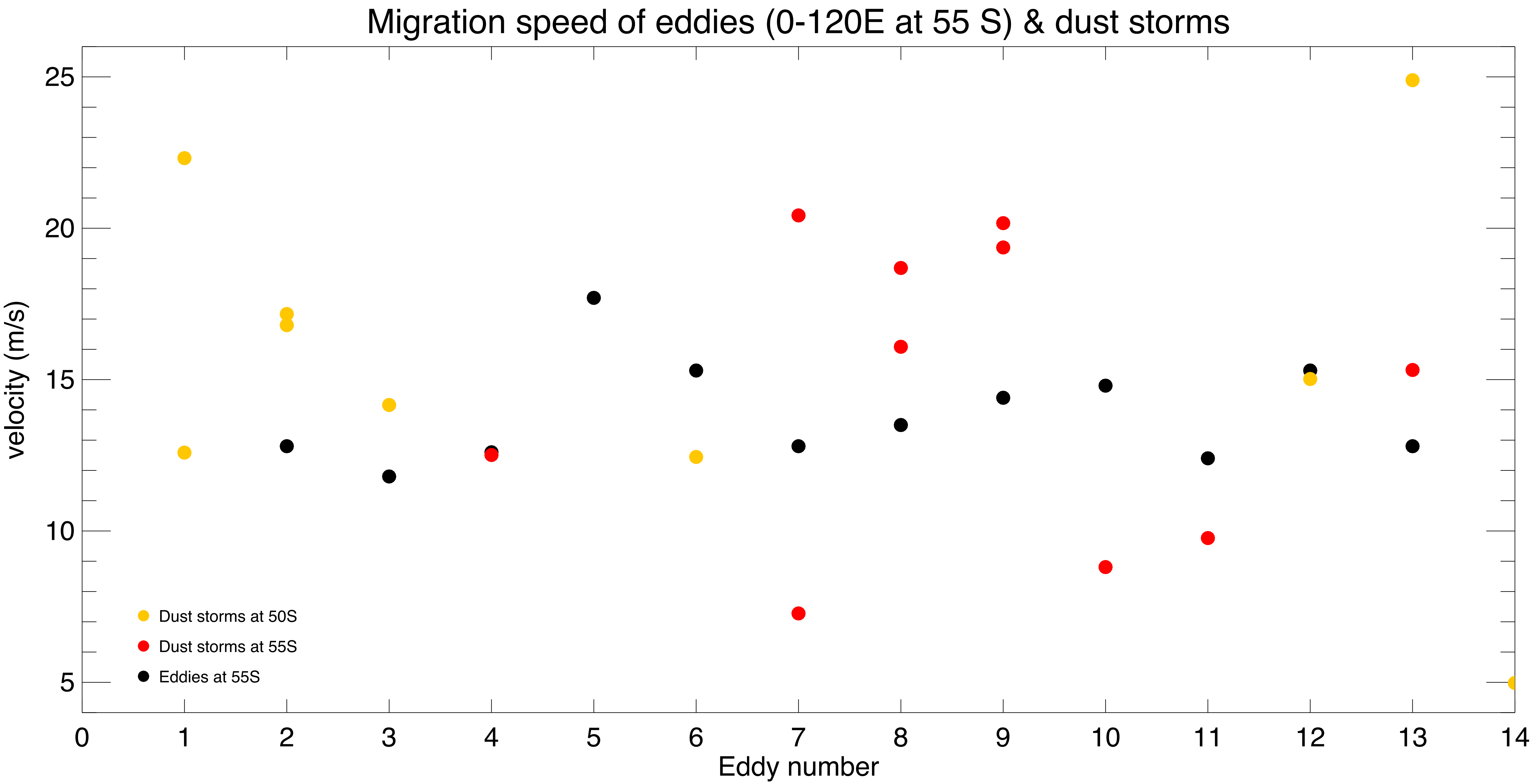

Periodicity – eddies & storms

Eddy #	Eddy period at 55S, 45 E (sols)	Storm period 30–60 E (sols)	Latitude of storm period (S)
1	——	——	
2	4.2	3	50
3	3.3	4	50
4	3.0	3	50
5	3.2	4	50
6	2.4		
7	3.1		
8	2.3		
9	3.1	3	55 & 50
10	2.8	3	55 & 51
11	2.7	2	55
12	3.4	4	55
13	3	2	55
14	——	——	——

Cold fronts

Although to first order we would locate cold fronts between cold (negative) and warm (positive) FFSM anomalies, their exact location cannot be determined from FFSM eddies alone – pressure and wind data are also required.

- The limited longitudinal resolution of TES data, and subsequent binning of FFSM data into 5 longitudinal bins, preclude precise determination of the location of cold fronts. Fronts are most intense close to the surface, but TES data averaging over the lowest scale height reduces their signal.
- Furthermore, we would expect a phase shift between eddy temperature and pressure fields, since isobaric and isosteric surfaces intersect under baroclinic conditions.
- The nature of Martian baroclinic waves and frontogenesis is understudied and consequently fronts have not been sufficiently investigated.

Dust lifting associated with eastward-travelling baroclinic eddies (SH)

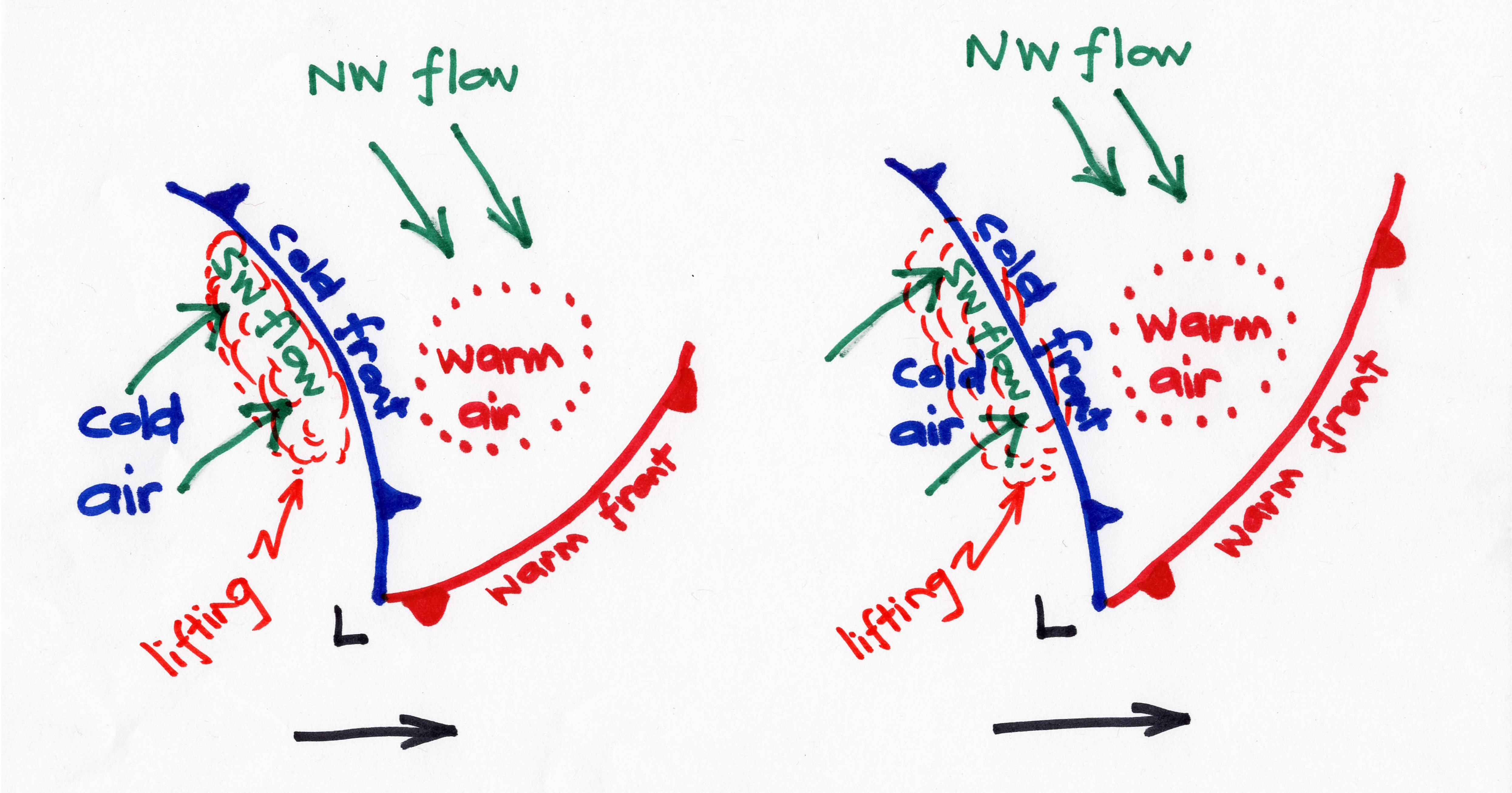

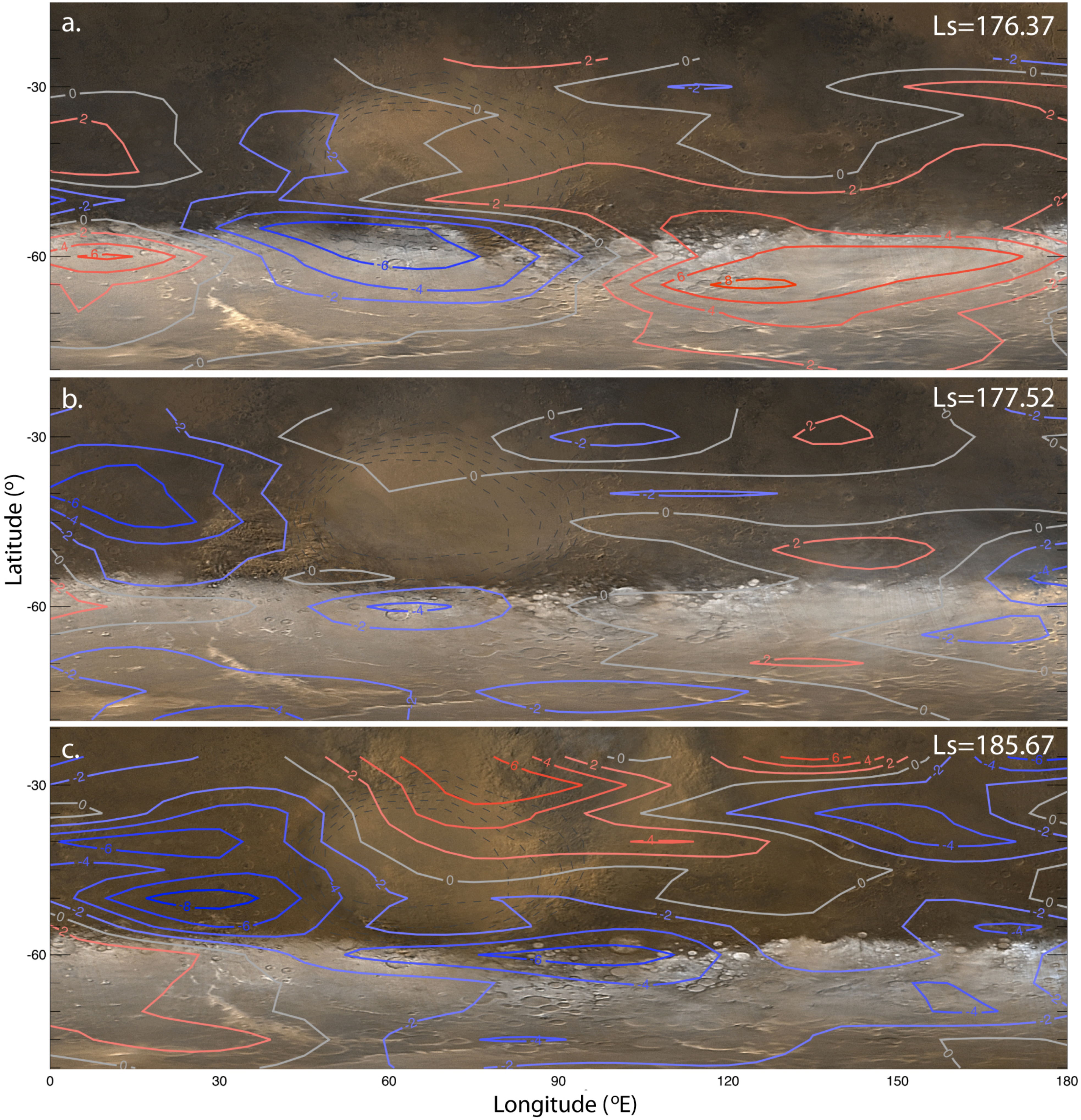
a.
Ls=176.37
b.
Ls=177.52
c.
Ls=185.67
-30
-60
Latitude (°)
0
30
60
90
120
150
180
Longitude (°E)

Eddy 8

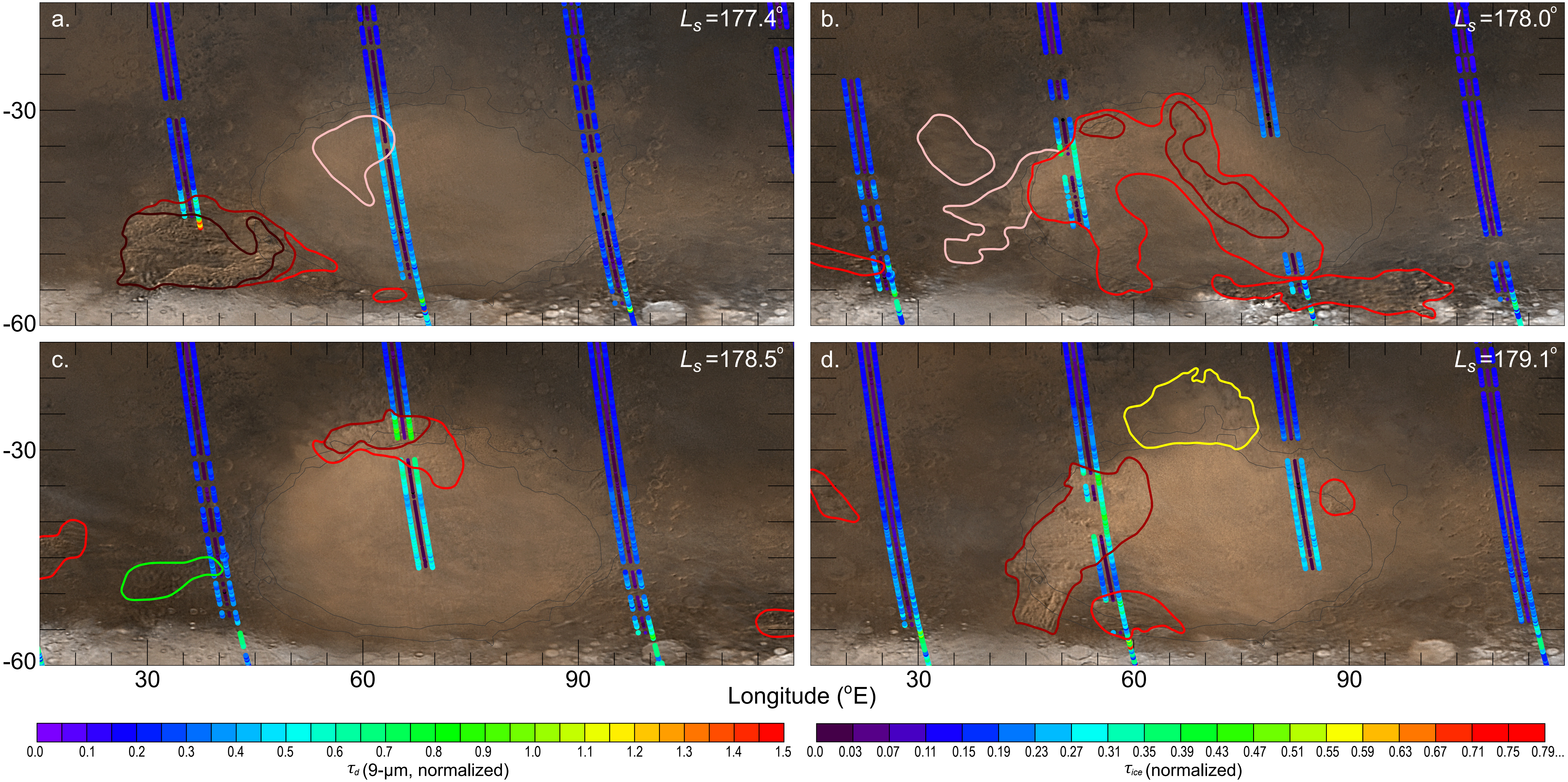
a.
Ls =177.4°
b.
Ls =178.0°
c.
Ls =178.5°
d.
Ls =179.1°
-30
-60
-30
-60
30
60
90
30
60
90
Longitude (°E)
0.0
0.1
0.2
0.3
0.4
0.5
0.6
0.7
0.8
0.9
1.0
1.1
1.2
1.3
1.4
1.5
τd (9-μm, normalized)
0.0
0.03
0.07
0.11
0.15
0.19
0.23
0.27
0.31
0.35
0.39
0.43
0.47
0.51
0.55
0.59
0.63
0.67
0.71
0.75
0.79...
τice (normalized)

Eddy 11

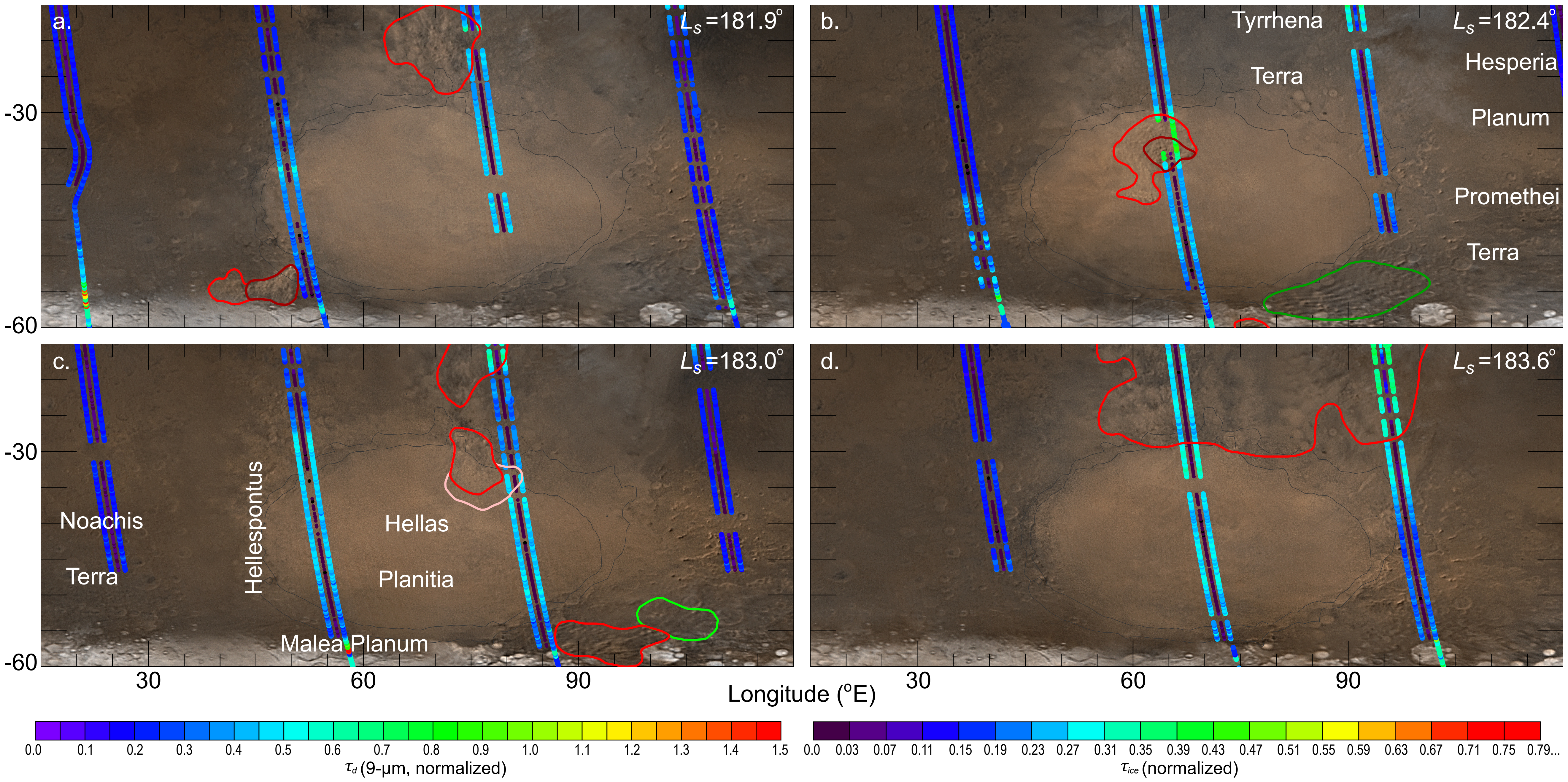
a.
L_s=181.9°
b.
L_s=182.4°
Tyrrhena
Terra
Hesperia
Planum
Promethei
Terra
c.
L_s=183.0°
Noachis
Terra
Hellespontus
Hellas
Planitia
Malea Planum
d.
L_s=183.6°
-30
-60
30
60
90
Longitude (°E)
0.0 0.1 0.2 0.3 0.4 0.5 0.6 0.7 0.8 0.9 1.0 1.1 1.2 1.3 1.4 1.5
τ_d (9-μm, normalized)
0.0 0.03 0.07 0.11 0.15 0.19 0.23 0.27 0.31 0.35 0.39 0.43 0.47 0.51 0.55 0.59 0.63 0.67 0.71 0.75 0.79...
τ_{ice} (normalized)

MY 24 – 26

TES FFSM eddies & MOC storms, 3.7 hPa, 60° S, MY 24, L_s=165.35-187.83°

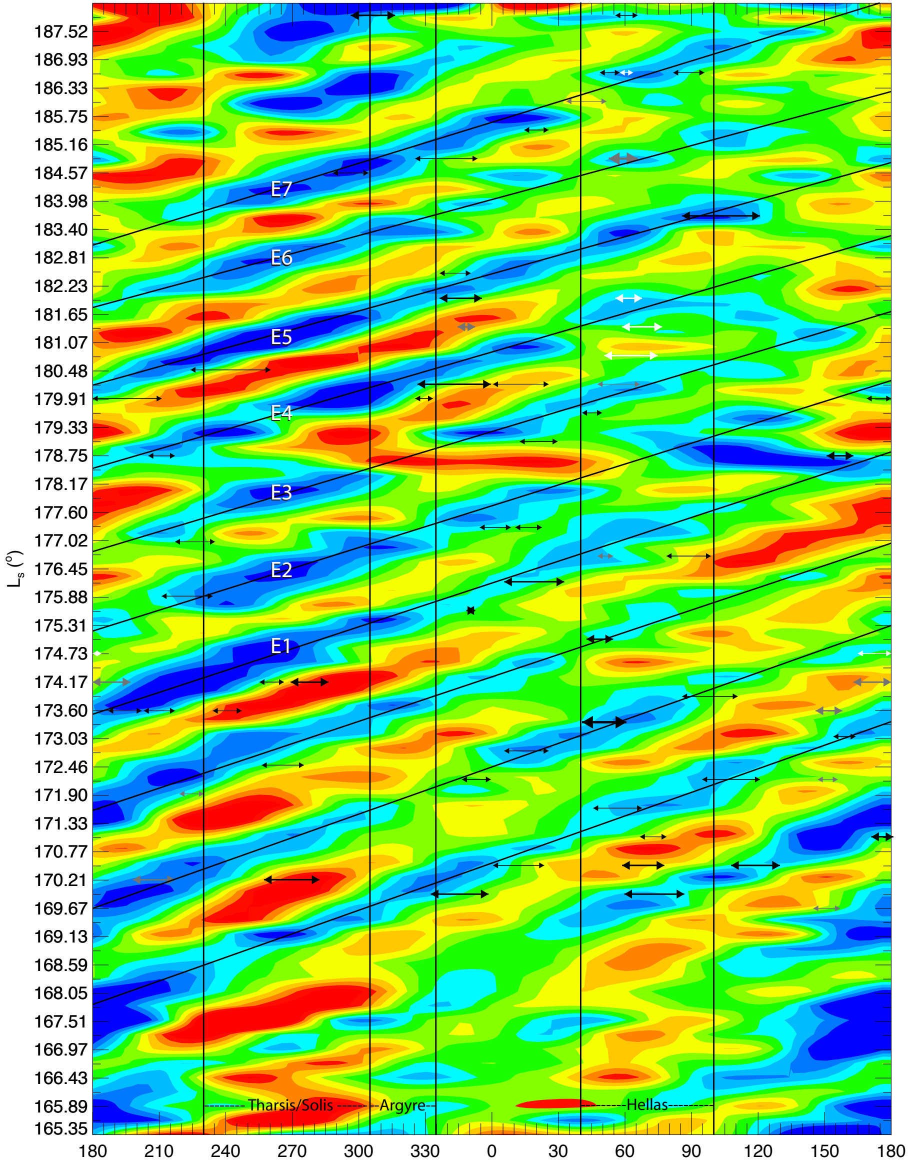

TES FFSM eddies & MOC storms, 3.7 hPa, 60° S, MY 25, L_s=165.0-187.74°

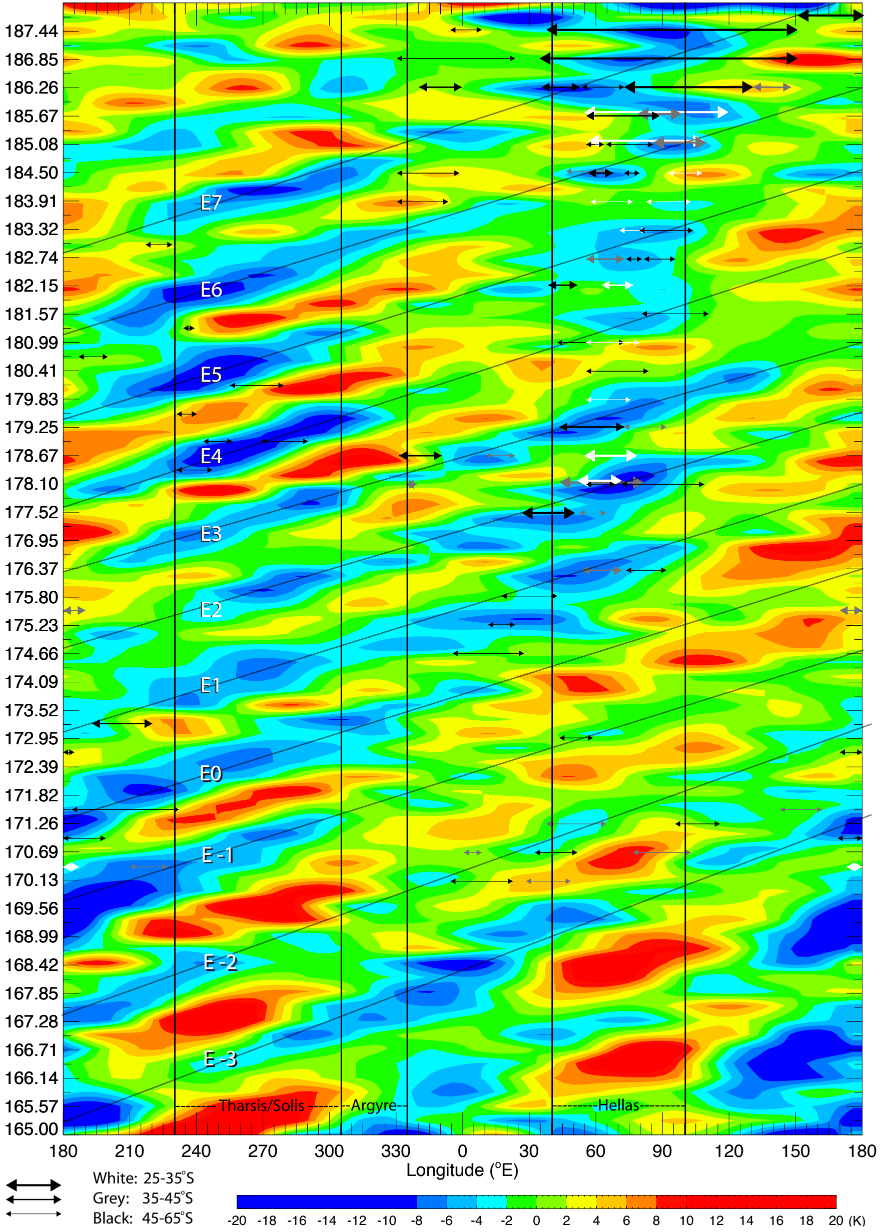

TES FFSM eddies (3.7 hPa, 60° S) & MOC visible dust storms, MY 26, L_s=175.14-192.42°

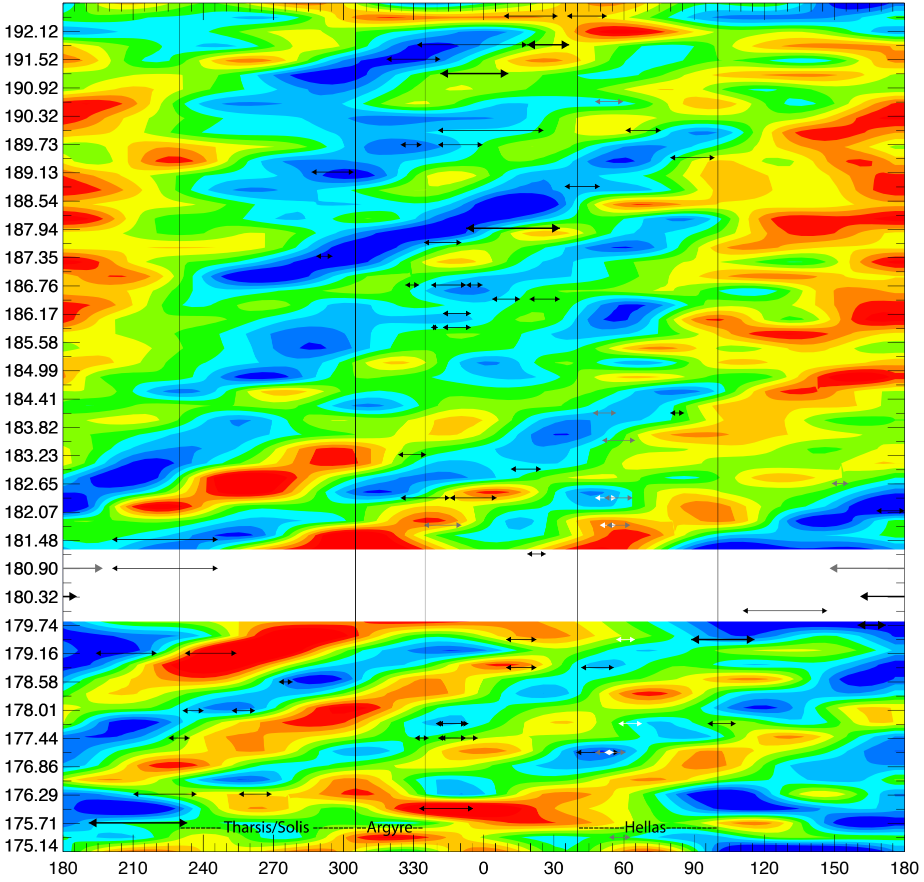

Working Hypothesis

We hypothesize that the sustained series of high-amplitude eddies in MY 25 was a factor in generating the PDS.

Six eastward-traveling baroclinic eddies triggered the precursor storms due to the enhanced dust lifting associated with their low-level wind and stress fields.

- Subsequent eddies contributed to storm expansion on Ls=186.3 and beyond

- The higher amplitudes seen in the FFSM temperature field is suggestive of higher-amplitude eddies in general. These would have had higher-amplitude low-level wind and stress fields associated with them, and could have led to more dust lifting (assuming the same amount of dust available to lift).

- It is possible that other interannual differences in transient eddy activity were involved in MY 25 PDS genesis (such as very shallow disturbances (Barnes 2010), but these could not have been detected by TES.

- Surface dust inventory is an important non-dynamical factor that can influence PDS interannual variability (Kahre et al. 2006).

Discussion – Eddy & storm associations

- Integration of MOC-observed dust storms and FFSM eddies shows:
  - concurrent eastward migration of eddies and dust storms, with:
    - similar migration speeds
    - similar periodicity

These associations suggest an eddy component in storm initiation

Discussion – Additional circulation components

Additional circulation components that may play a role in storm initiation include:

- cap-edge sublimation winds
- topographically-enhanced winds in the Hellas basin
- thermal tides

Discussion – Resolution limitations

Both the limited meteorological data and its coarse resolution

- constrains the depth of analysis
- precludes drawing firm conclusions about storm initiation, expansion, and interannual differences.

It is not possible to assess:

- spatial relationship between storms and eddy cold fronts
- the influence of various circulation components on MY 25 PDS genesis with the available MGS data.

Summary

- 42 MY 25 maps created (Ls=165.1 – 187.5)

  - available in NetCDF format for model input

- Integration of MOC-observed dust storms and FFSM eddies suggests concurrent eastward migration of dust storms and eddies (MY 24 – 26)

- Six eastward-traveling baroclinic eddies contributed to the initiation of MY 25 precursor storms due to enhanced dust lifting associated with their low-level wind and stress fields.

- Subsequent eddies contributed to MY 25 storm expansion on Ls=186.3 and beyond